

# Characteristics of iron status, oxidation response, and DNA methylation profile in response to occupational iron oxide nanoparticles exposure

Toxicology and Industrial Health  
2020, Vol. 36(3) 170–180  
© The Author(s) 2020  
Article reuse guidelines:  
sagepub.com/journals-permissions  
DOI: 10.1177/0748233720918683  
journals.sagepub.com/home/tih  


Min Yu<sup>1</sup> , Xingfan Zhou<sup>2</sup>, Li Ju<sup>1</sup>, Man Yu<sup>1</sup>,  
Xiangjing Gao<sup>3</sup>, Meibian Zhang<sup>3</sup> and Shichuan Tang<sup>2</sup>

## Abstract

Although the growing development and application of iron oxide nanoparticles (IONPs) may pose exposure risk and adverse health outcomes, biological changes due to occupational exposure remain unexplored. This cross-sectional study recruited 23 workers at a plant that manufactures IONPs and 23 age- and sex-matched controls without metal-rich occupational hazards exposure. Exposure metrics at worksites were monitored, and iron status, oxidation markers, and methylation profiles of genomic DNA in peripheral blood were measured using corresponding enzyme-linked immunosorbent assays and methylation-specific polymerase chain reaction (PCR), respectively. The mass concentration, number counting, and surface area concentration of airborne particles at the worksite significantly increased during the work process of manufacturing/handling IONPs. Overall, compared to controls, workers exhibited increased 5-hydroxymethylcytosine (5hmC) levels without changes in 5-methylcytosine (5mC), hepcidin methylation, iron, soluble transferrin receptor (sTfR), ferritin, hepcidin, 8-hydroxydeoxyguanosine, and glutathione. A positive correlation was found between 5hmC and IONP exposure year with adjustment for age, sex, and cotinine using partial correlation analyses ( $r = 0.521$ ,  $p < 0.001$ ). After stratification of IONPs exposure and 5hmC levels, the univariate general linear model with adjustment for age, sex, and cotinine found that the estimated mean levels of 5mC and sTfR in subjects with low and high 5hmC levels among controls were 11% and 14.4% ( $p \leq 0.01$ ) and 80.9 nM and 70.3 nM ( $p < 0.05$ ), respectively. The estimated mean levels of sTfR in workers and controls with low 5hmC levels were 88.3 nM and 68.7 nM ( $p \leq 0.01$ ). Multivariate linear regression analyses suggested an association between sTfR and 5hmC (standardized  $\beta = -0.420$ ,  $p = 0.014$ ) and female sex (standardized  $\beta = 0.672$ ,  $p < 0.001$ ) for subjects with low 5hmC levels. These findings suggest that increased 5hmC could be differentially employed to monitor an epigenetic signature with steady iron homeostasis for occupational IONP-exposed individuals who are likely to experience early but specific decreased sTfR, especially for females concurrent with the onset of increment in 5hmC at low level.

## Keywords

DNA methylation, iron oxide nanoparticles, occupational exposure, oxidation, soluble transferrin receptor

Received 13 September 2019; Revised 20 February 2020; Accepted 14 March 2020

<sup>1</sup>Department of Occupational Diseases, Zhejiang Academy of Medical Sciences, Hangzhou, Zhejiang, People's Republic of China

<sup>2</sup>Beijing Municipal Institute of Labor Protection, Beijing, People's Republic of China

<sup>3</sup>Zhejiang Provincial Center for Disease Control and Prevention, Hangzhou, Zhejiang, People's Republic of China

## Corresponding authors:

Min Yu, Department of Occupational Diseases, Zhejiang Academy of Medical Sciences, No. 182 Tianmushan Rd, Hangzhou, Zhejiang, People's Republic of China.

Email: yumin06@hotmail.com

Shichuan Tang, Beijing Municipal Institute of Labor Protection, No. 55 Taoranting Rd, Beijing, People's Republic of China.

Email: tsc3496@sina.com

## Introduction

Iron oxide nanoparticles (IONPs) are produced by chemical, physical, and biological methods, exhibit distinct physical and chemical characteristics, and are employed in many fields, such as medicine, environmental remediation, agriculture, and industry (Ali et al., 2016). At workplaces, IONPs may not only introduce exposure risks for workers at production and postsynthesis stages but also contaminate the air environment during cleaning and maintenance (Ding et al., 2017). Aerosol IONPs at worksites that manufacture IONPs are likely to exist at higher numbers and surface area levels under manual or semiautomatic operations than at sites without such activities (Xing et al., 2015; Zou et al., 2015). Insufficient control strategies may not appropriately control IONPs emission (Babik et al., 2018). Accordingly, IONPs are increasingly a source of hazard for at-risk workers, and the potential for adverse biological effects and/or toxicity remains critical (Kornberg et al., 2017).

Inhaled IONPs into the lungs may either undergo elimination through lung-associated lymph nodes or pass through the alveolar-capillary barrier into the circulation, which increases the risk for local and systemic toxicity (Sutunkova et al., 2016; Zhu et al., 2009). IONP-induced toxicity involves the extent of iron release and oxidative stress that is accompanied by reduced antioxidant activity and the formation of the indirect DNA damage marker 8-hydroxydeoxyguanosine (8-OHdG) (Laffon et al., 2018; Valdiglesias et al., 2016). In addition to oxidation indices, iron transport mediators were also involved as a response to IONPs in a rodent experiment (Yang et al., 2015). The metabolic pathway of inhaled IONPs likely involves transferrin and ferritin (Arami et al., 2015), the latter of which plays a role in regulating IONP degradation in a physiological relevant *in vitro* environment (Volatron et al., 2017). Nevertheless, the impact of IONPs on iron status and oxidant response markers has not yet been elucidated for individuals with occupational exposure.

Global and/or loci-specific DNA methylation signatures varied with different nanoparticle and biological systems (Wong et al., 2017). The global DNA methylation indices 5-methylcytosine (5mC) and 5-hydroxymethylcytosine (5hmC) can be differentiated with an enzyme-linked immunosorbent assays (ELISA) in particulate matter exposure research (Sanchez-Guerra et al., 2015). 5hmC is derived from 5mC oxidation, which is likely mediated by iron ion

and oxidant responses (Dao et al., 2014). The major regulator of systemic iron homeostasis and iron excess relevant oxidation is hepcidin, which appears to be regulated by DNA methylation (Gozzelino and Arosio, 2016; Sharp et al., 2018). The global and iron sensor gene-specific DNA methylation patterns require further investigation because of the scarcity of data on IONP-induced DNA methylation (Brzoska et al., 2019).

This study aimed to characterize global and hepcidin-loci-specific DNA methylation patterns and to elucidate the possible effect of DNA methylation signature on iron status and oxidant markers in IONP-exposed workers. Thus, this study may facilitate knowledge on IONP-induced epigenetic modification of biological effects in the real world.

## Materials and methods

### Subjects

The selection criteria of the investigated IONP-exposed workers in this cross-sectional study were as follows: (1) individuals who could experience exposure to IONPs during the work process, (2) individuals who did not have hematology and pulmonary abnormality, and (3) individuals who could provide peripheral blood samples. Accordingly, 23 first-line employees were recruited as workers in a plant that manufactures ferric oxide nanoparticles. As documented in our previous study, this environment thus poses a contamination risk of Fe and O elements-enriched airborne aerosols with spindle-like morphology and unimodal size distribution around 10–15 nm (Xing et al., 2015). Each worker was matched to a control individual from another plant who did not handle and/or produce nanomaterials, based on gender, age (difference  $\leq 3$  years), without metal-rich particulate matter and/or hazards exposure history at the worksite, and with no hematology and pulmonary abnormalities. Thus, 23 age- and sex-matched controls were ultimately selected. Next, peripheral blood samples from these 46 subjects were collected during a routine annual occupational medicine screening program, and their anticoagulated whole blood and serum were from whole blood without an anticoagulant stored at  $-80^{\circ}\text{C}$  until further analyses.

### Analysis of exposure metrics

Sampling was performed before and during the work process of manufacturing/handling IONPs at the

worksite to determine the exposure metrics levels, including mass concentration in  $\text{mg}/\text{m}^3$ , number counting in  $\text{particles}/\text{m}^3$ , and surface area concentration in  $\mu\text{m}^2/\text{cm}^3$ , according to a monitoring strategy and instrument that is described previously (Xing et al., 2015). Briefly, DustTrak 8530 (TSI, Shoreview, Minnesota, USA), P-TRAK 8525 (TSI), and Aero-Trak™ 9000 (TSI) instruments were employed for 30 min at the worksite prior or during the work process to characterize mass concentration of particles that ranged from 100 nm to 1000 nm, number counting of particles that ranged from 20 nm to 1000 nm, and surface area concentration of particles that ranged from 10 nm to 1000 nm, respectively.

### *Iron status parameter measurements*

The iron concentration in units of  $\mu\text{M}$  was determined using 500  $\mu\text{L}$  of serum and a serum iron assay kit, which is based on the reaction between ferrous iron and dipyrindine according to the manufacturer's instructions (Beijing BioRab Tech Co. Ltd., China). Hepcidin, ferritin, and soluble transferrin receptor (sTfR) levels were measured with 10  $\mu\text{L}$  of serum in 40  $\mu\text{L}$  of dilution buffer, as suggested in the corresponding protocol for each ELISA kit (Jiangsu MeiMian Industrial Co. Ltd., China). The corresponding minimum detectable concentrations were 1.0  $\text{ng}/\text{mL}$ , 0.1  $\text{ng}/\text{mL}$ , and 0.1  $\text{nM}$ , respectively.

### *DNA methylation profile analyses*

Genomic DNA was extracted from 200  $\mu\text{L}$  of whole blood using a Blood Genomic DNA Mini Kit (cwbiotech, China). DNA (100 ng per sample) was coated onto the wells of each plate, followed by blocking with anti-5mC and secondary antibody incubation, color development, and absorbance measurement at 450 nm, according to the 5-mC quantification instruction of the 5-mC DNA ELISA kit (Zymo Research, Irvine, California, USA).

For quantification of 5hmC, after the anti-5hmC polyclonal antibody coating and blocking process in each well of the 96-well plate, 100 ng of DNA per sample was subjected to DNA binding, anti-DNA horseradish peroxidase (HRP) antibody incubation, color development, and absorbance detection at 405 nm, as instructed by the protocol of Quest 5-hmC™ DNA ELISA Kit (Zymo Research).

Hepcidin gene methylation levels were determined using methylation-specific polymerase chain reaction (PCR). Briefly, methylation (M)- and nonmethylation

(U)-specific primers that corresponded to a hepcidin sequence that ranged from 192 bp to 1292 bp were designed using MethPrimer (Li and Dahiya 2002) and are described as follows: hepcidin (M): (left): 5'-TTTTATTTTTTAGGGTTGTGGTTTC-3', (right): 5'-CCAATTATTAATCTTATCCCTCCG-3', and the amplification length was 173 bp; hepcidin (U): (left): 5'-TTTATTTTTTAGGGTTGTGGTTTTG-3', (right): 5'-CAATTATTAATCTTATCCCTCCACC-3', and the amplification length was 171 bp. Then, 200 ng of DNA was subjected to bisulfite conversion using a Methylamp™ DNA Modification Kit (Epi-gentek, Farmingdale, New York, USA). Modified DNA (2  $\mu\text{L}$ ) was employed for PCR reaction at 56.4°C and 53.9°C to anneal the M and U primers, respectively. The PCR cycles were set to 40 in a Thermal Cycler according to the instructions of Zymo Taq™ DNA Polymerase (Zymo Research). Next, unmethylated and methylated PCR products of each DNA sample from the matched controls and workers simultaneously underwent electrophoresis in the same 2% agarose gel, followed by measurements of band intensity using Image J software (NIH, Bethesda, Maryland, USA) with the same analyzed region size, similar background adjustment, and the same band intensity reading criteria. Lastly, the methylation percentage per sample was calculated as follows:  $M\% = 100 \times (\text{the intensity of M PCR product}/\text{the sum of intensity of M and U products})$ .

### *Evaluation of oxidation response indices*

The 8-OHdG and glutathione levels were determined using 10  $\mu\text{L}$  of serum in 40  $\mu\text{L}$  of dilution buffer as suggested in the corresponding ELISA kits (Jiangsu MeiMian Industrial Co. Ltd.). The minimum detectable concentration of 8-OHdG and glutathione was 0.1  $\text{ng}/\text{mL}$  and 0.1  $\mu\text{M}$ , respectively. A 50  $\mu\text{L}$  aliquot of 5-fold diluted serum was mixed with 100  $\mu\text{L}$  of HRP-conjugated reagent in the selected wells in a 96-well plate, followed by incubation at 37°C for 60 min, washing using wash solution, color development using 100  $\mu\text{L}$  of tetramethylbenzidine substrate solution, reaction termination with 50  $\mu\text{L}$  of stop solution that contains sulfuric acid, and absorbance reading at 450 nm, according to the corresponding instruction of 8-OHdG and glutathione ELISA kit.

### *Cotinine concentration determination*

The Cotinine ELISA kit (Abnova, China), which is a solid-phase competitive ELISA that has a minimum

**Table 1.** Baseline information of IONP-exposed workers and nonexposed controls.<sup>a</sup>

	Controls (n = 23)	Workers (n = 23)	p Value	
Age (years)	47 (39–50)	46 (40–51)	0.869	
Female (n, %)	13, 26.5%	13, 26.5%	1.000	
Work history (year) <sup>b</sup>	—	2.0 (0.5–2.5)	—	
Number counting <sub>20–1000 nm</sub> (10 <sup>5</sup> /cm <sup>3</sup> ) <sup>c</sup>	—	0.11 (0.09–0.12) <sup>d</sup>	0.36 (0.32–0.48) <sup>e</sup>	<0.001 <sup>f</sup>
Mass concentration <sub>100–1000 nm</sub> (mg/m <sup>3</sup> ) <sup>c</sup>	—	0.04 (0.04–0.05) <sup>d</sup>	0.24 (0.24–0.26) <sup>e</sup>	<0.001 <sup>f</sup>
Surface area concentration <sub>10–1000 nm</sub> (μm <sup>2</sup> /cm <sup>3</sup> ) <sup>c</sup>	—	81.77 (80.46–83.75) <sup>d</sup>	169.90 (133.40–208.30) <sup>e</sup>	<0.001 <sup>f</sup>
Cotinine (ng/mL)	0.88 (0.26–6.30)	0.57 (0–31.46)	0.581	

IONP: iron oxide nanoparticles.

<sup>a</sup>Data are presented as median (interquartile range<sub>25–75</sub>) or number with percentage. —: not applicable.

<sup>b</sup>The year at worksite in a plant that manufactures ferric oxide nanoparticle.

<sup>c</sup>Mass concentration of particles that range from 100 nm to 1000 nm, number counting of particles that range from 20 nm to 1000 nm, and surface area concentration of particles that range from 10 nm to 1000 nm, respectively.

<sup>d</sup>Background measurements for 30 min before the work process of manufacturing/handling IONPs at worksite for workers.

<sup>e</sup>Measurements during the work process of manufacturing/handling IONPs for 30 min at worksite for workers.

<sup>f</sup>p Value was determined between measurement d and e.

detectable level of 1 ng/mL, was used to measure cotinine concentration in 10 μL of serum, according to the manufacturer's protocol. Briefly, 10 μL of undiluted serum was added to the selected wells of a 96-well plate and then mixed with 100 μL of the enzyme conjugate, followed by incubation at room temperature for 60 min, washing with wash buffer, mixing with 100 μL of substrate reagent, reaction terminating using 100 μL of stop solution, and absorbance measurement at 450 nm.

### Statistical analysis

The qualitative data are presented as numbers and percentages and were compared using  $\chi^2$  tests. The quantitative data are presented as median with interquartile range<sub>25–75</sub>. The cutoff points of 5hmC were determined using interquartile<sub>50</sub> of each group, followed by the indicated analysis when applicable. Comparisons between the two groups were performed with Mann–Whitney *U* tests. Correlation coefficients between variables were determined using partial correlation analysis with adjustments for age, sex, and cotinine. To further exclude the possible impact of age, sex, and cotinine on variables changes, general linear regression (univariate) was used to estimate variable levels. Next, the efficiency of age, sex, cotinine, 5hmC, and INOPs exposure history in predicting candidate variables was determined using multivariate linear regression analysis with stepwise method when applicable. All analyses were carried out with IBM SPSS Statistic version 22 and GraphPad Prism

version 6.0, and  $p < 0.05$  was considered as statistically significant.

### Results

The median duration of the working period was 2.0 years for workers with occupational IONP exposure, and their median age, sex, and mean cotinine levels were comparable to their counterparts (controls) who did not experience IONP exposure. Meanwhile, increased levels of mass concentration, number counting, and surface area concentration of airborne particles were observed during the work process of manufacturing/handling IONPs (Table 1).

Iron, sTfR, ferritin, and hepcidin concentrations in sera were comparable between workers and controls (Figure 1). Significantly greater 5hmC median levels in workers were found than in controls, but no significant differences in 5mC, hepcidin gene methylation, 8-OHdG, and glutathione levels were found (Figure 2).

Table 2 summarizes the feature of DNA methylation profile, iron status, and oxidative response indices stratified by interquartile range<sub>50</sub> level of 5hmC of controls and workers. Within controls, significantly higher 5mC levels were found in subjects with high 5hmC levels than the others with low 5hmC levels. Additionally, significantly higher 5mC levels were found in workers than controls with low 5hmC levels. Nevertheless, no other investigated indices significantly varied in subgroup analyses.

Overall, a positive correlation between working history and 5hmC was found after adjusting for

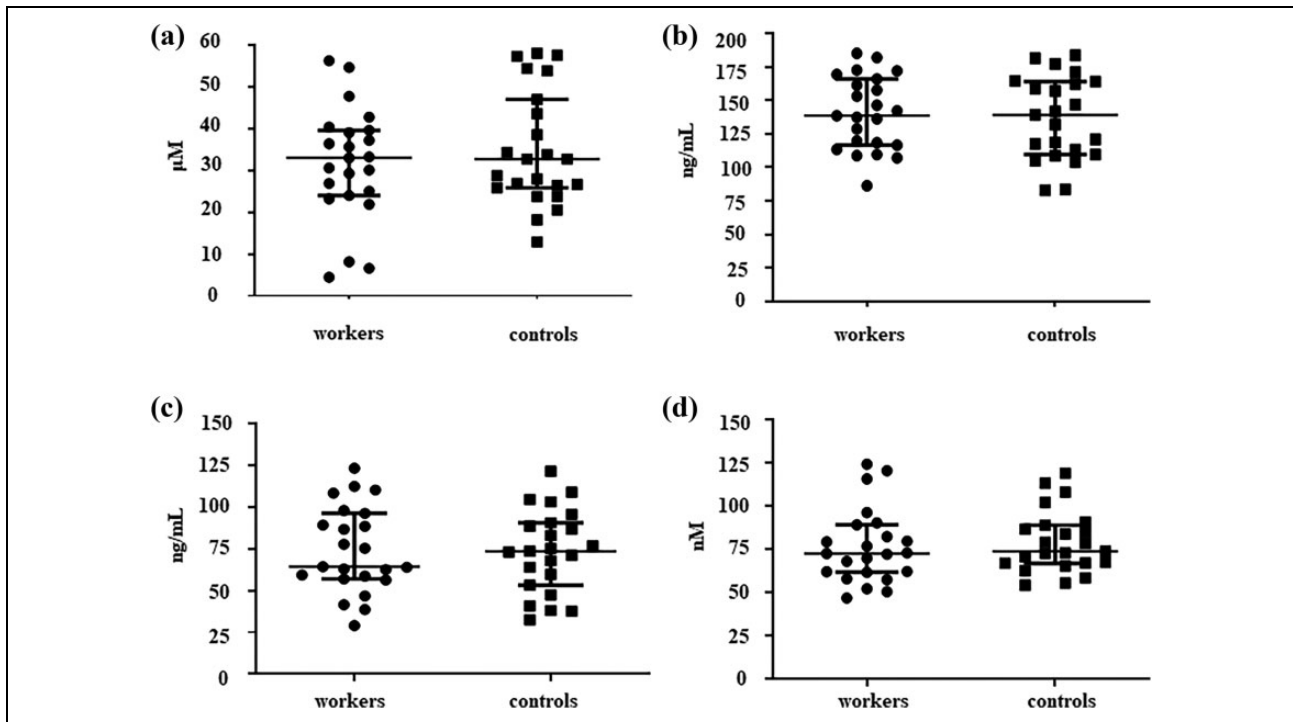


**Figure 1.** Measurements of serum iron status markers in IONP-exposed workers and nonexposed controls. (a) Iron, (b) hepcidin, (c) ferritin, and (d) sTfR. The error bar indicates median and interquartile range<sub>25–75</sub>. IONP: iron oxide nanoparticles; sTfR: soluble transferrin receptor.

cotinine, age, and sex in partial correlation analyses that included both workers and controls, although no significant relationship between working history and 5hmC among workers was evident. Meanwhile, 5hmC was positively correlated with 5mC and negatively correlated with sTfR in controls (Table 3). Moreover, the univariate general linear model with adjustments for cotinine, age, and sex showed that significantly lower estimated mean levels of 5mC and significantly higher estimated mean levels of sTfR were found in subjects with low 5hmC levels than the others with high 5hmC levels within controls, respectively. Intriguingly, the estimated mean level of sTfR was significantly less in workers than controls for subjects with low 5hmC levels (Table 4). Additional multivariate linear regression analyses indicated that 5hmC, age, sex, and cotinine were not associated with sTfR, although 5hmC (standardized  $\beta = 0.526$ ,  $p = 0.004$ ) and age (standardized  $\beta = 0.422$ ,  $p = 0.018$ ) correlated with 5mC for controls (adjusted  $R^2 = 0.414$ ,  $p = 0.002$ ). Meanwhile, reduced sTfR levels were associated with increased 5hmC (standardized  $\beta = -0.420$ ,  $p = 0.014$ ) and female sex (standardized  $\beta = 0.672$ ,  $p < 0.001$ ) for subjects with low 5hmC levels (adjusted  $R^2 = 0.461$ ,  $p = 0.001$ ).

## Discussion

To our knowledge, this is the first field report that suggests that inhaled IONPs can increase 5hmC without affecting 5mC, iron sensor gene loci DNA methylation, or oxidant markers. sTfR reduction concurrent with onset of increment in 5hmC might be observed for subjects, especially for females even at low 5hmC levels, which provides a tentative iron metabolic marker for monitoring IONP-exposed workers with specific global DNA methylation patterns.

Both acute and chronic IONP exposure via the respiratory tract cause alveolar cell damage and epithelial–blood barrier impairment (Park et al., 2015; Srinivas et al., 2012), which may facilitate IONP translocation between its primary deposited organ and the blood through a diffusion mechanism, especially for particulates with small size and high penetrability (Sutunkova et al., 2018). Meanwhile, IONPs likely release iron ions when they encounter biological fluid that is derived from the lung or blood (Sutunkova et al., 2018). Intravenous injection of IONPs to rats increased plasma iron concentrations, which persisted for at least 120 days and were concurrent with elevated plasma ferritin and reduced transferrin (Milto et al., 2014). Increased ferritin and

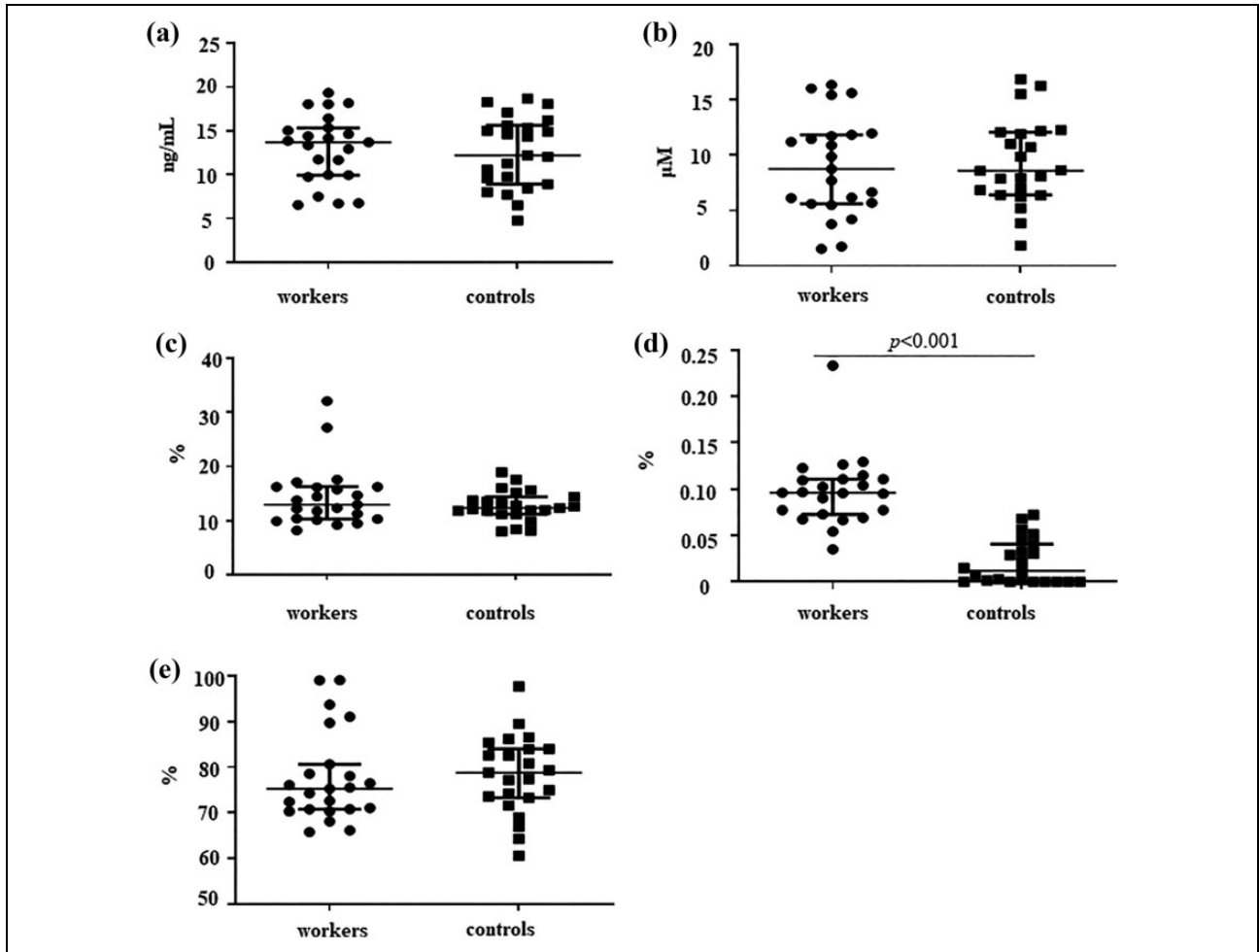


**Figure 2.** Oxidation response markers and DNA methylation profile in peripheral blood in IONP-exposed workers and nonexposed controls. (a) Glutathione, (b) 8-OHdG, (c) 5mC, (d) 5hmC, and (e) hepcidin gene methylation level. The error bar indicates median and interquartile range<sub>25–75</sub>. IONP: iron oxide nanoparticles; 5hmC: 5-hydroxymethylcytosine; 5mC: 5-methylcytosine; 8-OHdG: 8-hydroxydeoxyguanosine.

reduced TfR levels were observed in an IONP-exposed macrophage model, and the increased ferritin, which was localized near particulate aggregates, was noted in mice that were injected with IONPs (Rojas et al., 2017). The availability of metallic nanoparticles in the body may differ based on the exposure routes, in which injection generally has higher bioavailability than inhalation with a proposed rate approaching 5% (Lin et al., 2015). The low pulmonary bioaccessibility of iron has been attributed to the absent impact of an occupation (e.g. welding) that involves respiratory iron exposure on serum biomarkers suggestive of iron status, such as hepcidin and ferritin (Casjens et al., 2014). However, iron metabolic indices in response to occupational intrapulmonary IONP exposure are still lacking. In rats with single-dose intratracheal exposure of IONPs during

a 50-day observation period, a rapid and sharp increase in blood iron levels occurred within 1 week, followed by a declining trend (Zhu et al., 2009). Herein, without consideration, the DNA methylation patterns, neither serum iron nor ferritin, hepcidin, or sTfR, showed significant changes in workers who were at worksites with aerosol IONP contamination for an extended period, which is consistent with the concept that abnormal levels of iron metabolic markers are transient and persist no longer than 4 days for healthy volunteers with bronchial instillation of iron oxide (Ghio et al., 1998).

Occupational aerosol IONP exposure seems to increase the levels of oxidation markers, including 8-OHdG, in exhaled breath condensate, but not in urine (Pelclova et al., 2016) or in serum as reported in the present study. Inhaled IONP-induced oxidation

**Table 2.** Characteristics of DNA methylation profile, iron status, and oxidative response indices in IONP-exposed workers and nonexposed controls by 5hmC levels.<sup>a</sup>

	Controls		Workers				p Value <sup>d</sup>	p Value <sup>e</sup>
	5hmC (%)		5hmC (%)					
	Low (n = 11)	High (n = 12)	Low (n = 13)	High (n = 10)	p Value <sup>b</sup>	p Value <sup>c</sup>		
Iron ( $\mu\text{M}$ )	26.9 (23.8–34.3)	35.6 (26.8–56.6)	33.0 (23.6–38.2)	31.9 (24.3–44.0)	0.151	0.648	0.569	0.418
Hepcidin (ng/mL)	139.3 (108.9–159.0)	144.6 (114.6–169.7)	157.9 (111.6–172.6)	136.9 (119.1–148.3)	0.316	0.343	0.252	0.497
Ferritin (ng/mL)	73.1 (63.9–88.5)	74.4 (42.5–94.3)	63.9 (49.2–92.7)	82.2 (61.0–101.5)	0.833	0.313	0.424	0.381
sTfR (nM)	84.4 (67.1–82.6)	71.7 (65.7–82.6)	68.1 (57.7–80.8)	76.3 (67.9–101.2)	0.190	0.186	0.119	0.381
Glutathione (ng/mL)	12.2 (8.0–16.2)	13.2 (9.1–15.3)	14.4 (10.8–17.2)	12.5 (7.3–14.1)	0.976	0.208	0.531	0.539
8-OHdG ( $\mu\text{M}$ )	8.6 (6.8–11.0)	9.0 (6.4–12.2)	6.2 (4.8–11.6)	10.7 (6.4–12.7)	0.740	0.343	0.649	0.974
5mC (%)	11.8 (8.4–12.1)	14.1 (12.4–16.0)	13.8 (10.2–16.7)	12.3 (10.3–16.2)	0.001	0.738	0.047	0.346
Hepcidin gene methylation (%)	82.6 (78.8–85.4)	73.9 (69.6–81.2)	76.1 (70.5–85.9)	74.8 (70.7–79.8)	0.059	0.879	0.186	0.771

IONP: iron oxide nanoparticles; 5hmC: 5-hydroxymethylcytosine; 5mC: 5-methylcytosine; sTfR: soluble transferrin receptor; 8-OHdG: 8-hydroxydeoxyguanosine.

<sup>a</sup>The low and high 5hmC cutoff point levels were determined using interquartile<sub>50</sub> values of controls and workers, respectively. Data are expressed as median (interquartile range<sub>25–75</sub>).

<sup>b</sup>Comparison between subjects with low and high 5hmC levels within controls.

<sup>c</sup>Comparison between subjects with low and high 5hmC levels within workers.

<sup>d</sup>Comparison between controls and workers with low 5hmC level.

<sup>e</sup>Comparison between controls and workers with high 5hmC level.

**Table 3.** Correlation efficiencies between 5hmC and working history, iron status, and oxidative response indices in IONP-exposed workers and nonexposed controls.

	Working history	5mC	Hepcidin gene methylation	Iron	Hepcidin	Ferritin	sTfR	Glutathione	8-OHdG
<b>5hmC<sup>a</sup></b>									
<i>r</i>	0.521	0.245	−0.059	−0.094	0.099	0.054	−0.123	0.031	0.014
<i>p</i>	<0.001	0.114	0.707	0.551	0.527	0.730	0.431	0.843	0.930
<b>5hmC<sup>b</sup></b>									
<i>r</i>	—	0.476	<0.001	−0.057	0.426	−0.256	−0.671	0.396	−0.309
<i>p</i>		0.034	0.999	0.812	0.061	0.276	<0.001	0.084	0.185
<b>5hmC<sup>c</sup></b>									
<i>r</i>	−0.040	0.019	−0.187	−0.027	−0.135	0.231	0.171	−0.290	0.250
<i>p</i>	0.867	0.935	0.431	0.909	0.570	0.328	0.472	0.215	0.287

IONP: iron oxide nanoparticles; Working history: the year at worksite in a plant that manufactures ferric oxide nanoparticle; 5mC: 5-methylcytosine; 5hmC: 5-hydroxymethylcytosine; sTfR: soluble transferrin receptor; GSH: glutathione; 8-OHdG: 8-hydroxydeoxyguanosine; —: not applicable.

<sup>a</sup>Results were determined using partial correlation analyses with adjustments for age, sex, and cotinine in both controls and workers.

<sup>b</sup>Results were determined using partial correlation analyses with adjustments for age, sex, and cotinine in controls.

<sup>c</sup>Results were determined using partial correlation analyses with adjustments for age, sex, and cotinine in workers.

appears to be readily and sensitively detectable in the airway, which is a primary deposited site, rather than in the circulation or excretory system of the body. Moreover, the lack of evidently dysregulated levels of iron and iron metabolic indices in the circulation system of participants who were exposed to IONPs, as found by the present study, contrasts the proposed mechanism underlining IONP-induced oxidative stress and dysregulated interaction between labile iron pool and iron regulation players (Kornberg et al., 2017), which partially contribute to the unchanged 8-OHdG levels. Meanwhile, the reserved level of GSH, which prevents oxidation and DNA damage, might also counter against unfavorable 8-OHdG changes (Abu-Shakra and Zeiger, 1997; Kart et al., 2016).

A previous field report (Liou et al., 2017) and the current data demonstrate the capacity of indium tin oxide and silica, but not titanium oxide and IONPs, to induce global DNA hypomethylation, which supports the concept that discrepant epigenetic effects are induced by occupational metal oxide nanoparticles that are exposed to different chemical composition (Sierra et al., 2016). IONP-exposed, but not nonexposed, individuals failed to verify the positive association between 5mC and 5hmC, regardless of hazards exposure (e.g. metal and ambient air pollution) (Sanchez-Guerra et al., 2015; Tellez-Plaza et al., 2014), which suggest the possible modification of nanoparticles in the relationship between 5hmC and 5mC. Herein, IONP exposure differentially increased

5hmC, while 5mC remained unchanged. Enhanced 5hmC was due to *in vitro* labile iron pool augmentation (Camarena et al., 2017), which did not occur for IONP exposure-enhanced 5hmC *in vivo* because no changes in iron status were observed. High 5hmC level was consistently identified for IONP-exposed, as compared to nonexposed individuals, even in the presence of low 5hmC levels. In addition, elevated 5hmC and female sex appeared to be indicators of sTfR reduction. IONP-exposed individuals potentially experience reduced sTfR, especially in females, even with relatively lower 5hmC content. The possible role of 5hmC in the active demethylation process and/or stress response (Shi et al., 2017) is unlikely to explain the sTfR changes through 5hmC-mediated iron sensor gene dysmethylation mechanism due to the lack of association between 5hmC and hepcidin methylation. The detailed biological meaning of decreased sTfR for IONP-exposed individuals with low 5hmC remains elusive but may partially reflect the disrupted new iron metabolic equilibrium due to an undertermined interaction between sTfR and iron transferrin (Schreinemachers and Ghio, 2016; Speeckaert et al., 2010).

The IONP exposure determination (yes/no) in this study is a binary variable that is based on the year of working history and provides no personal exposure quantification. Nevertheless, the exposure metrics analyzed in this study during the work process of manufacturing/handling IONPs indicate the possibility of IONP release. Meanwhile, the comprehensive

**Table 4.** Estimated mean value with 95% confidence interval of sTfR and 5mC in IONP-exposed workers and nonexposed controls by 5hmC levels.<sup>a</sup>

	Controls		Workers		Controls		Workers	
	5hmC (%)		5hmC (%)		5hmC (%)		5hmC (%)	
	Low (n = 11)	High (n = 12)	Low (n = 13)	High (n = 10)	Low (n = 11)	Low (n = 13)	High (n = 12)	High (n = 10)
sTfR (nM)	89.0 (76.9–101.1)	70.3 <sup>b</sup> (58.8–81.7)	75.6 (67.3–84.0)	77.8 (68.1–87.4)	88.3 (78.2–98.3)	68.7 <sup>c</sup> (59.5–77.8)	74.4 (64.8–84.0)	82.7 (72.2–92.2)
5mC (%)	11.0 (9.5–12.4)	14.4 <sup>d</sup> (13.0–15.8)	13.5 (10.3–16.7)	15.4 (11.7–19.1)	10.7 (8.0–13.4)	14.4 (12.0–16.9)	14.1 (11.2–16.9)	14.8 (11.7–17.9)

IONP: iron oxide nanoparticles; 5hmC: 5-hydroxymethylcytosine; 5mC: 5-methylcytosine; sTfR: soluble transferrin receptor.

<sup>a</sup>The estimated values of variables were determined using general linear regression (univariate) including age, sex, and cotinine as covariates; the low and high 5hmC cutoff point levels were determined using interquartile<sub>50</sub> values of controls and workers, respectively. Data are presented as median (interquartile range<sub>25–75</sub>).

<sup>b</sup>Comparison of sTfR level between subjects with low and high 5hmC levels within controls ( $p < 0.05$ ).

<sup>c</sup>Comparison of sTfR level between controls and workers with low 5hmC level ( $p \leq 0.01$ ).

<sup>d</sup>Comparison of 5mC level between subjects with low and high 5hmC levels within controls ( $p \leq 0.01$ ).

iron metabolic markers that were reported in this study may reflect certain internal chemical composition-specific indices changes. Although methylation-specific PCR with gel image analysis is a sensitive and convenient method for rapid detection of DNA methylation of a locus of interest in bodily fluids (Ramalho-Carvalho et al., 2018), the hepcidin methylation status in peripheral blood measured here was semiquantitative. Further comprehensive methods with absolute hepcidin methylation measurements are warranted. Moreover, the nature of the cross-sectional design with limited sample size precludes causal interpretations. Nevertheless, the present study extends our knowledge regarding metal nanoparticles-induced epigenetic changes as explored with comparable sample sizes (Liou et al., 2017) and necessitates further investigations recruiting larger population with longer-term observations.

## Conclusion

Elevated 5hmC may be differentially employed to monitor an epigenetic signature with steady iron homeostasis in occupational IONP-exposed individuals, who are likely to experience early but specific decreases in sTfR, especially for females concurrent with the onset of increment in 5hmC at low levels.

## Data availability

All the results are available in text. Further query of the raw data is achievable in the journal.

## Declaration of conflicting interests

The author(s) declared no potential conflicts of interest with respect to the research, authorship, and/or publication of this article.

## Ethical approval and informed consent

All the procedures in this study are in consistent with the requirement of amended Helsinki Declaration of 1983, which is approved by the ethical committee of the Beijing Municipal Institute of Labor Protection and performed with the verbal consent obtained from the participants.

## Funding

The author(s) disclosed receipt of the following financial support for the research, authorship, and/or publication of this article: This study was financially supported by Open Foundation of the Key Laboratory of Occupational Safety and Health, Beijing Municipal Institute of Labour Protection (2018).

**ORCID iD**

Min Yu  <https://orcid.org/0000-0002-5909-1475>

**References**

- Abu-Shakra A and Zeiger E (1997) Formation of 8-hydroxy-2'-deoxyguanosine following treatment of 2'-deoxyguanosine or DNA by hydrogen peroxide or glutathione. *Mutation Research* 390(1–2): 45–50.
- Ali A, Zafar H, Zia M, et al. (2016) Synthesis, characterization, applications, and challenges of iron oxide nanoparticles. *Nanotechnology Science and Application* 9: 49–67.
- Arami H, Khandhar A, Liggitt D, et al. (2015) In vivo delivery, pharmacokinetics, biodistribution and toxicity of iron oxide nanoparticles. *Chemical Society Reviews* 44(23): 8576–8607.
- Babik KR, Dahm MM, Dunn KH, et al. (2018) Characterizing workforces exposed to current and emerging non-carbonaceous nanomaterials in the U.S. *Journal of Occupational and Environmental Hygiene* 15(1): 44–56.
- Brzoska K, Gradzka I, and Kruszewski M (2019) Silver, gold, and iron oxide nanoparticles alter miRNA expression but do not affect DNA methylation in HepG2 cells. *Materials (Basel, Switzerland)* 12(7): E1038.
- Camarena V, Sant DW, Huff TC, et al. (2017) cAMP signaling regulates DNA hydroxymethylation by augmenting the intracellular labile ferrous iron pool. *eLife* 6: e29750.
- Casjens S, Henry J, Rihs HP, et al. (2014) Influence of welding fume on systemic iron status. *The Annals of Occupational Hygiene* 58(9): 1143–1154.
- Dao T, Cheng RY, Revelo MP, et al. (2014) Hydroxymethylation as a novel environmental biosensor. *Current Environmental Health Reports* 1(1): 1–10.
- Ding Y, Kuhlbusch T, Van Tongeren M, et al. (2017) Airborne engineered nanomaterials in the workplace—a review of release and worker exposure during nanomaterial production and handling processes. *Journal of Hazardous Materials* 322(Pt A): 17–28.
- Ghio AJ, Carter JD, Richards JH, et al. (1998) Disruption of normal iron homeostasis after bronchial instillation of an iron-containing particle. *The American Journal of Physiology* 274(3): L396–L403.
- Gozzelino R and Arosio P (2016) Iron homeostasis in health and disease. *International Journal of Molecular Sciences* 17(1): E130.
- Kart A, Koc E, Dalginli KY, et al. (2016) The therapeutic role of glutathione in oxidative stress and oxidative DNA damage caused by hexavalent chromium. *Biological Trace Element Research* 174(2): 387–391.
- Kornberg TG, Stueckle TA, Antonini JA, et al. (2017) Potential toxicity and underlying mechanisms associated with pulmonary exposure to iron oxide nanoparticles: conflicting literature and unclear risk. *Nanomaterials (Basel, Switzerland)* 7(10): E307.
- Laffon B, Fernandez-Bertolez N, Costa C, et al. (2018) Cellular and molecular toxicity of iron oxide nanoparticles. *Advances in Experimental Medicine and Biology* 1048: 199–213.
- Li LC and Dahiya R (2002) Methprimer: designing primers for methylation PCRS. *Bioinformatics (Oxford, England)* 18(11): 1427–1431.
- Lin Z, Monteiro-Riviere NA, and Riviere JE (2015) Pharmacokinetics of metallic nanoparticles. *Wiley Interdisciplinary Reviews. Nanomedicine and Nanobiotechnology* 7(12): 189–217.
- Liou SH, Wu WT, Liao HY, et al. (2017) Global DNA methylation and oxidative stress biomarkers in workers exposed to metal oxide nanoparticles. *Journal of Hazardous Materials* 331: 329–335.
- Milto IV, Grishanova AY, Klimenteva TK, et al. (2014) Iron metabolism after application of modified magnetite nanoparticles in rats. *Biochemistry (Moscow)* 79(11): 1245–1254.
- Park EJ, Oh SY, Lee SJ, et al. (2015) Chronic pulmonary accumulation of iron oxide nanoparticles induced th1-type immune response stimulating the function of antigen-presenting cells. *Environmental Research* 143(Pt A): 138–147.
- Pelcova D, Zdimal V, Kacer P, et al. (2016) Oxidative stress markers are elevated in exhaled breath condensate of workers exposed to nanoparticles during iron oxide pigment production. *Journal of Breath Research* 10(1): 016004.
- Ramalho-Carvalho J, Henrique R, and Jerónimo C (2018) Methylation-specific PCR. *Methods in Molecular Biology (Clifton, N.J.)* 1708: 447–472.
- Rojas JM, Gavilan H, Del DV, et al. (2017) Time-course assessment of the aggregation and metabolization of magnetic nanoparticles. *Acta Biomaterialia* 58: 181–195.
- Sanchez-Guerra M, Zheng Y, Osorio-Yanez C, et al. (2015) Effects of particulate matter exposure on blood 5-hydroxymethylation: results from the Beijing truck driver air pollution study. *Epigenetics* 10(7): 633–642.
- Schreinemachers DM and Ghio AJ (2016) Effects of environmental pollutants on cellular iron homeostasis and ultimate links to human disease. *Environmental Health Insights* 10: 35–43.
- Sharp PA, Clarkson R, Hussain A, et al. (2018) DNA methylation of hepatic iron sensing genes and the regulation of hepcidin expression. *PLoS One* 13(5): e197863.

- Shi DQ, Ali I, Tang J, et al. (2017) New insights into 5hmc DNA modification: generation, distribution and function. *Frontiers in Genetics* 8: 100.
- Sierra MI, Valdes A, Fernandez AF, et al. (2016) The effect of exposure to nanoparticles and nanomaterials on the mammalian epigenome. *International Journal of Nanomedicine* 11: 6297–6306.
- Speeckaert MM, Speeckaert R, and Delanghe JR (2010) Biological and clinical aspects of soluble transferrin receptor. *Critical Reviews in Clinical Laboratory Sciences* 47(5–6): 213–228.
- Srinivas A, Rao PJ, Selvam G, et al. (2012) Oxidative stress and inflammatory responses of rat following acute inhalation exposure to iron oxide nanoparticles. *Human & Experimental Toxicology* 31(11): 1113–1131.
- Sutunkova MP, Katsnelson BA, Privalova LI, et al. (2016) On the contribution of the phagocytosis and the solubilization to the iron oxide nanoparticles retention in and elimination from lungs under long-term inhalation exposure. *Toxicology* 363–364: 19–28.
- Sutunkova MP, Privalova LI, Minigalieva IA, et al. (2018) The most important inferences from the Ekaterinburg nanotoxicology team's animal experiments assessing adverse health effects of metallic and metal oxide nanoparticles. *Toxicology Reports* 5: 363–376.
- Tellez-Plaza M, Tang WY, Shang Y, et al. (2014) Association of global DNA methylation and global DNA hydroxymethylation with metals and other exposures in human blood DNA samples. *Environmental Health Perspectives* 122(9): 946–954.
- Valdiglesias V, Fernandez-Bertolez N, Kilic G, et al. (2016) Are iron oxide nanoparticles safe? Current knowledge and future perspectives. *Journal of Trace Elements in Medicine and Biology* 38: 53–63.
- Volatron J, Carn F, Kolosnjaj-Tabi J, et al. (2017) Ferritin protein regulates the degradation of iron oxide nanoparticles. *Small* 13(2): 1602030.
- Wong B, Hu Q, and Baeg GH (2017) Epigenetic modulations in nanoparticle-mediated toxicity. *Food and Chemical Toxicology* 109(Pt 1): 746–752.
- Xing M, Zhang Y, Zou H, et al. (2015) Exposure characteristics of ferric oxide nanoparticles released during activities for manufacturing ferric oxide nanomaterials. *Inhalation Toxicology* 27(3): 138–148.
- Yang L, Kuang H, Zhang W, et al. (2015) Size dependent biodistribution and toxicokinetics of iron oxide magnetic nanoparticles in mice. *Nanoscales* 7(2): 625–636.
- Zhu MT, Feng WY, Wang Y, et al. (2009) Particokinetics and extrapulmonary translocation of intratracheally instilled ferric oxide nanoparticles in rats and the potential health risk assessment. *Toxicological Sciences* 107(2): 342–351.
- Zou H, Zhang Q, Xing M, et al. (2015) Relationships between number, surface area, and mass concentrations of different nanoparticles in workplaces. *Environmental Science. Processes & Impacts* 17(8): 1470–1481.